Published in final edited form as:
Science. 1990 December 14; 250(4987): 1541–1546.

Interfacial Catalysis: The Mechanism of Phospholipase A_2

David L. Scott,
Department of Molecular Biophysics and Biochemistry and the Howard Hughes Medical Institute, Yale University, New Haven, CT 06511

Steven P. White,
Department of Molecular Biophysics and Biochemistry and the Howard Hughes Medical Institute, Yale University, New Haven, CT 06511

Zbyszek Otwinowski,
Department of Molecular Biophysics and Biochemistry and the Howard Hughes Medical Institute, Yale University, New Haven, CT 06511

Wei Yuan,
Departments of Chemistry and Biochemistry, University of Washington, Seattle, WA 98195

Michael H. Gelb, and
Departments of Chemistry and Biochemistry, University of Washington, Seattle, WA 98195

Paul B. Sigler
Department of Molecular Biophysics and Biochemistry and the Howard Hughes Medical Institute, Yale University, New Haven, CT 06511

Abstract

A chemical description of the action of phospholipase A_2 (PLA_2) can now be inferred with confidence from three high-resolution x-ray crystal structures. The first is the structure of the PLA_2 from the venom of the Chinese cobra (*Naja naja atra*) in a complex with a phosphonate transition-state analogue. This enzyme is typical of a large, well-studied homologous family of PLA_2s. The second is a similar complex with the evolutionarily distant bee-venom PLA_2. The third structure is the uninhibited PLA_2 from Chinese cobra venom. Despite the different molecular architectures of the cobra and bee-venom PLA_2s, the transition-state analogue interacts in a nearly identical way with the catalytic machinery of both enzymes. The disposition of the fatty-acid side chains suggests a common access route of the substrate from its position in the lipid aggregate to its productive interaction with the active site. Comparison of the cobra-venom complex with the uninhibited enzyme indicates that optimal binding and catalysis at the lipid-water interface is due to facilitated substrate diffusion from the interfacial binding surface to the catalytic site rather than an allosteric change in the enzyme's structure. However, a second bound calcium ion changes its position upon the binding of the transition-state analogue, suggesting a mechanism for augmenting the critical electrophile.

Phospholipase A_2 (PLA_2) is a paradigm for calcium - mediated enzymatic reactions at a lipid-aqueous interface because its hydrolytic activity toward the 2-acyl group (hence the

---

Note added in proof: Since this paper was accepted, Thunnissen *et al.* [*Nature* **347**, 689 (1990)] have published a 2.4 Å crystal structure of a complex containing a genetically modified form of porcine pancreatic PLA_2 and an *sn-2* amide phospholipid analogue. The interactions of the calcium ion with the *sn-3* phosphate and the *sn-2* carbonyl, as well as the orientation of the *sn-1* and *sn-2* alkyl substituents, are consistent with those of the diC_8(2Ph)PE derivatives discussed here. However, the *trans* planar amide is accommodated by forming a hydrogen bond between the amide NH and the Nδ1 of His48. This interaction may explain the unusually strong affinity of this competitive inhibitor, but—as the authors state—it does not clarify the mechanism.

designation A_2) of *L*-1,2 diacylphosphatides is directed preferentially against substrate aggregates such as micelles, monolayers, vesicles, or membranes. Interest in the action of PLA_2 also derives from its implication in mediating the inflammatory response through the release of arachidonic acid from the *sn-2* position of phospholipids in the plasma membrane. Arachidonate is the precursor of the eicosanoid mediators of inflammation including leukotrienes, thromboxanes, and prostaglandins. Secreted PLA_2s are convenient for biochemical and biophysical studies as they are rugged small proteins (usually about 120 to 134 amino acids) that can be easily purified in large amounts from pancreatic juice and the venom of snakes and insects. The protein is readily crystallized in well-ordered lattices and has been cloned from a wide variety of cDNA libraries. Two of these clones and their mutational variants have been overexpressed and studied biochemically and crystallographically (1).

The action of PLA_2 has been exhaustively reviewed but there is little consensus on the details of catalysis or the molecular basis for this enzyme's strong preference for lamellar or micellar substrate. In this article, we propose a mechanism for the action of PLA_2. Our proposals for both the binding mechanism and the chemistry of catalysis are based primarily on the recently reported 2.0 Å crystal structures of two PLA_2 complexes with a phosphonate transition-state analogue. One complex is formed with PLA_2 from the venom of the Chinese cobra (2), which is a member of a large homologous family of PLA_2s referred to as the Class I/II family (3). The other complex is formed with the evolutionarily divergent PLA_2 from bee venom (4). In both cases the inhibitor is *L*-1-*O*-octyl-*2*-heptylphosphonyl-*sn*-glycero-*3*-phosphoethanolamine [diC_8(2Ph)PE] (Fig. 1).

The stereochemical picture of PLA_2 catalysis is completed by the 1.5 Å crystal structure of the uninhibited *N. n. atra* enzyme (Fig. 2). This structure enables us to answer important questions relating to structural adjustments in both the protein and its ligands caused by the binding and hydrolysis of substrate. Specifically, this structure enables us to see that (i) stabilizing the transition-state complex involves preservation of the coordination geometry of the primary calcium ion—two calcium-associated water molecules from the uninhibited enzyme are displaced by the oxyanion of the substrate's tetrahedral intermediate and the nonbridging oxygen of the *sn-3* phosphate; (ii) stabilization of the transition state may involve recruitment of additional positive charge to neutralize the oxyanion of the tetrahedral intermediate; and (iii) there are no conformational adjustments in the backbone required to optimize substrate binding or catalysis.

Catalytic mechanism

The formation, stabilization, and collapse of the transition state is schematically outlined in Fig. 3. In this mechanism we assume that the phosphonate emulates the tetrahedral intermediate of esterolysis whose formation, stability, and productive collapse are fostered by the enzyme's catalytic surface. The interactions of the phosphonate with the enzyme's catalytic functionalities are shown in Fig. 4. One of the nonbridging phosphonate oxygens is hydrogen bonded to the Nδ1 of the active site His48(34) (5, 6) and represents the attacking hydroxyl produced by the histidine's abstraction of a proton from a water molecule found at the same position in the uninhibited form of the *N. n. atra* venom PLA_2 (Fig. 2). A water molecule is found at this position in all high-resolution crystal structures of Class I/II PLA_2s (7). Since no acyl enzyme intermediate has been observed, this water was invoked as the likely source for the nucleophile to attack the carbonyl function (6, 8). The proton abstracted by His48(34) is only 2.6 Å from the bridging *sn-2* oxygen and is therefore ideally situated to protonate this oxygen in concert with the productive collapse of the tetrahedral intermediate (9). The nonbridging oxygen of the phosphonate facing the calcium ion represents the oxyanion of the tetrahedral intermediate formed from the substrate carbonyl by nucleophilic

attack and interacts with the calcium ion as one of its equatorial ligands. Thus the oxyanion is electrostatically stabilized by the calcium ion and a backbone amide N–H from Gly30(10) while satisfying the geometrical requirements for calcium coordination. During catalysis, the oxyanion, calcium ion, and attacking nucleophile are buried in the enzyme's interior where they are devoid of hydrogen bonds to solvent. The solvent's access to the active site is limited; the nearest fixed water molecule is at least 5 Å away from the attacking nucleophile. This exclusion of water from the active site is likely to strongly augment the electrostatic forces that stabilize the transition state.

Without benefit of direct structural evidence, Verheij *et al.* (6) suggested a formal mechanism that is remarkably close to that indicated by the structures of our transition-state analogue complexes. We propose that the active site His48(34) extracts a proton from a water molecule bound to the Nδ1 position (9). The extracted proton is perfectly positioned to be subsequently deposited on the alkoxide leaving group to provide a low-energy pathway that draws the collapse of the tetrahedral intermediate toward the desired products. The positive charge acquired by the enzyme when it abstracts the proton from the attacking water molecule is presumably stabilized through an extended hydrogen-bonded network that includes His48(34) and Asp99(64) (Fig. 2). This charge can then be readily "recalled" for protonation of the *sn-2* alkoxide.

This stereochemical device is reminiscent of the catalytic system of the serine proteases. There are three differences, however. First, in PLA_2 only water can serve as the source of the nucleophile. In the serine proteases, the active site serine is deprotonated to create a nucleophile in the acylation step. In the deacylation step of the serine protease mechanism, virtually any dispersed potential nucleophile (such as alcohol or hydroxylamine) can attack the carbonyl of the acyl enzyme. Second, tyrosines are present in the catalytic network of PLA_2; two are absolutely conserved in all Class I/II enzymes (Tyr52 and Tyr73). Tyr87 of the bee-venom PLA_2 forms the same hydrogen bond as Tyr52 of the *N. n atra* enzyme, but its ring is oriented differently since it arises from a nonanalogous backbone site. Although these Tyr residues extend the catalytic network by forming hydrogen bonds between their phenolic hydroxyls and the carboxylate of Asp99(64) of the catalytic network, site-directed mutational studies (10) have shown that the principal function of these tyrosines is to provide structural support. The catalytic network is further extended in the Class I/II family by a water molecule that links the amino terminus to the Oδ1 of the relay's Asp99(64) (Fig. 2). Third, the hydrogen-bonding patterns of the imidazole ring differ. Blow (11) points out that the catalytic triad of the serine proteases (12) and the pancreatic-microbial lipases (13) extracts a proton at the Nε2 of the active histidine, while the aspartate carboxylate of the catalytic network interacts through Nδ1. The opposite holds true in the case of PLA_2; Nδ1 generates the nucleophile and Nε2 interacts with the carboxylate of Asp99(64). Moreover, the interaction between His48(34) and the carboxylate of Asp99(64) involves a hydrogen bond in the *anti* rather than the *syn* conformation seen in the serine proteases. This is noteworthy because the *anti* lone pair is a much weaker base (~10^4 fold) than the *syn* lone pair (14).

The role of the calcium ion

Calcium ion is essential both for the binding of substrate and for catalysis. Figure 4 shows the coordination geometry of the calcium-ion cofactor in the two transition-state analogue complexes and in the uninhibited enzyme. As is the case for calcium-binding sites in other proteins (15), the ion is hepta-coordinated by a pentagonal bipyramidal cage of O atoms. The calcium ion unifies catalysis and binding by providing two ligation positions: one equatorial site for electrophilic stabilization of the oxyanion in the putative tetrahedral intermediate and one axial position for the pro-*S* nonbridging oxygen of the *sn-3* phosphate.

The former lowers the activation barrier of the transition state, and the latter aids substrate binding and chiral selection (16). In the uninhibited form of the *N. n atra* enzyme, as well as other PLA_2 structures of the Class I/II family (7), the sites used by the substrate's oxygens are occupied by the oxygens of two water molecules (17). As the substrate undergoes catalysis, the oxyanion and the *sn-3* phosphate clamp the calcium ion, each displacing a water molecule from the ligation cage. This displacement of water to the bulk solvent should help stabilize the transition-state interaction by an entropic factor. There should also be an enthalpic gain since the dipolar interactions of the water molecules are replaced with much stronger interactions involving the formally charged atoms of the substrate. The structures also suggest that, if prior to nucleophilic attack the scissile ester's carbonyl oxygen is coordinated by the electrophilic calcium, the ester would be required to rotate out of the plane defined by the trigonal carbonyl and the bridging oxygen. Whereas the strain caused by an out-of-plane deformation might be tolerated in the case of esters, it is likely to be prohibitively large for nitrogen-containing analogues like *sn-2* amides or carbamates. We suggest that because of their resistance to such deformation, these nitrogen-containing analogues cannot bind to the enzyme in the same productive conformation as the phosphonates and esters. This may account, at least in part, for the great resistance of such analogues to hydrolysis (18).

A supplemental electrophile

The mechanism described here relies mainly on the calcium ion to neutralize the oxyanion of the tetrahedral intermediate. However, the negative charges of Asp49 and the *sn-3* phosphate have already neutralized the calcium ion's positive charge even before the contribution of the oxyanion from the tetrahedral intermediate is considered. We have found that the uninhibited *N. n atra* PLA_2 has a second fully occupied hepta-coordinated calcium-binding site 11 Å from the primary site (derived from the side chains of Asp24 and Asn119). This site is not present in the transition-state analogue complexes; instead, there is a different secondary calcium ion bound 4.6 Å closer to the oxyanion (19). We propose that calcium binds to its "new" location during enzymatic action and is coordinated by O29, the carbonyl oxygen of the peptide formed with N30. From the interaction of the *sn-2* phosphonate, we have inferred, as shown schematically in Fig. 3, that the amido hydrogen of N30 interacts with the presumed oxyanion of the tetrahedral intermediate. Thus the newly positioned calcium ion can hyperpolarize the peptide and, in effect, focus its positive charge directly on the oxyanion. The occurrence of the secondary calcium ion in both complexes of the asymmetric unit suggests that it is physiologically significant (20). The coordination geometry of the primary calcium site may provide the precise scaffold for catalysis and the charge on the secondary calcium ion, focused by the C29–N30 peptide, may serve as a supplemental electrophile to stabilize the oxyanion. There are no kinetic or solution studies that bear directly on the function or even existence of this secondary calcium ion. If this mechanism is general for PLA_2, we should find either similar secondary calcium-binding sites in other crystal structures or other potentially mobile positive charges in the vicinity of the C29–N30 peptide. In this regard, we note that the crystal structure of bovine pancreatic PLA_2 (21) shows Lys122 interacting with O29 through an intervening water molecule, thereby also polarizing the peptide. The side chain of Lys122 (Cα to Nζ distance is 5.2 Å) is buckled, which suggests that the effect could be enhanced by expulsion of the intervening water and full extension of the Lys side chain (Cα to Nζ distance is 7.3 Å) to form a direct hydrogen bond. We found no evidence for a supplemental electrophile in the bee-venom complex.

The *sn-3* substituent—contribution to binding affinity

Phospholipids derive much of their identity from the nature of the moiety that forms the distal *sn-3* ester. Phosphatidylethanolamine derivatives are a common component of neutral membrane phospholipids. In the case of *N. n atra* PLA_2, the amino group of $diC_8(2Ph)PE$ forms a hydrogen bond with a surface asparagine. This interaction would presumably not occur with the quaternary ammonium group of choline. In the bee-venom enzyme, a similar interaction occurs with an unrefined portion of the carbohydrate. It is difficult to interpret the effect of *sn-3* esters on a PLA_2 substrate binding since the nature of the phosphatidyl ester also affects the physical chemistry of the aggregates (such as surface charge potential distribution or the state of aggregation).

The hydrophobic channel: access and stabilization of bound substrate

The *sn-1* and *sn-2* alkyl substituents lie roughly parallel in a hydrophobic channel that extends approximately 14 Å from the catalytic site to an opening just “above” the amino-terminal helix (residues 1 to 12) of the *N. n atra* enzyme and the functionally analogous third helix (residues 76 to 90) of the bee-venom enzyme (Fig. 5). The *sn-2* substituent is sharply bent at the tetrahedral phosphonate as in crystalline phospholipids (22). However, unlike the crystal structures of phospholipids, the *sn-3* substituents do not fold back over the *sn-2* esters but form specific polar interactions with the enzyme and its calcium-ion cofactor. The walls of the channel in both inhibited enzymes have been described (2, 4). The channel in both complexes has a dynamic feature that we believe facilitates diffusion of the phospholipid from the substrate aggregate into the active site of the enzyme without exposure to the solvent. The left wall of the channel is formed by a potentially mobile hydrophobic “flap” that is only secured firmly once the substrate is productively bound. In the *N. n atra* enzyme, this wall is the ring of Tyr69 whose phenolic hydroxyl is bound to the inhibitor’s *sn-3* phosphate, which in turn is firmly anchored to the primary calcium ion. Some members of the Class I/II family have a Lys69 residue, in which case the four methylene groups of this side chain probably form the hydrophobic left wall of the channel and the ε-amino group binds to the *sn-3* phosphate. In the bee-venom enzyme, the flexible left wall is provided by Arg57, which is also stabilized by the *sn-3* phosphate bound to the calcium ion.

The interfacial binding surface

If in both the *N. n atra* and bee-venom complexes the acyl chains of the inhibitor were lengthened to correspond to those of natural substrates, they would protrude well beyond the surface of the enzyme and their “free” termini would presumably remain embedded in the aggregate. In this way we infer that the interfacial binding surfaces are adjacent to the mouths of the hydrophobic channels (Fig. 5). In the case of Class I/II enzymes, the interfacial surface would include the first half of the amino-terminal helix, the usually hydrophobic side chain at position 19, and possibly the highly conserved Tyr75. This location is consistent with fluorescence and chemical protection studies, which show that Trp3 and Trp19, respectively, are involved in binding to aggregated substrate (23) and also readily explains why the pancreatic enzymes’ ability to bind and rapidly hydrolyze aggregated substrate (24) is dependent on the first half of the new amino-terminal helix created during the conversion from proenzyme to enzyme. In the case of the bee-venom PLA_2, the third helix (residues 76 to 90) is analogous to the amino-terminal helix of the Class I/II family and, although oriented differently, would also contribute side chains to the interfacial binding surface [see figure 3 in (4)].

Enzymatic action at the interface

PLA_2 is far more active at the lipid-aqueous interface than in solution. This phenomenon is termed "interfacial activation." The term is misleading because it implies that the normal basal function of the enzyme is activated when it encounters an aggregate. When viewed in this way it is natural to suggest that when the enzyme encounters the lipid-aqueous interface it undergoes a conformational change or oligomerization, or both, that enhances catalytic activity. However, PLA_2 has none of the properties of most allosteric systems; that is, this enzyme is extracellular, usually monomeric, and extremely robust, and its conformation is rigidly maintained by seven disulfide bridges (7). It is more accurate, and hence more useful, to state that PLA_2 is a soluble enzyme designed to attack the *sn-2* ester of aggregated phospholipids. The basal activity is to bind and digest lamellar and micellar aggregates of phospholipids. Activity against monomeric dispersed phospholipid would be a rare cellular event and constitutes a nearly irrelevant laboratory event.

Clearly, our crystals of the inhibited enzyme do not represent a true interfacial complex; indeed, it is unlikely that a crystal can be grown of a PLA_2–condensed substrate complex that would be sufficiently well ordered to reveal catalytic details. However, for reasons to be developed below, we believe that our transition-state analogue complexes present a structure that gives a fresh insight into the mechanism of interfacial lipolysis.

A commonly held view is that interfacial binding induces a favorable allosteric transition in the protein: the structural evidence argues against this. First of all, high-resolution crystal structures of PLA_2 have shown that the catalytic surface is exactly the same, regardless of the degree of evolutionary divergence, state of oligomerization, ionic strength, or pH of the crystallization conditions. Second, if one compares the two representations of the active site in the asymmetric unit of the inhibited form of the *N. n atra* enzyme and that seen in the crystalline complex with the bee-venom enzyme, the catalytic machinery and the portions of the inhibitor that contact the catalytic surface are essentially the same. It is extremely unlikely that there could be three identical arrangements in three different crystalline environments (one involving a widely divergent evolutionary homologue) unless that arrangement represented the most stable, and therefore the optimal, interaction between the transition state and the enzyme. Comparison of the uninhibited form of the *N. n atra* enzyme with either of its two transition-state analogue complexes in the crystalline asymmetric unit shows that the protein backbone and primary calcium site are virtually superimposable. If the structure of the transition-state inhibitor represents the optimal productive mode of binding, then no conformational changes are required of the protein backbone or its primary calcium site to achieve this optimal mode.

Third, three of the four water molecules consistently found bound to the catalytic surface in all refined, high-resolution crystal structures of uninhibited PLA_2 are displaced by O atoms of the transition-state analogue with perfect preservation of the pentagonal bipyramidal coordination of the calcium ion (25). The perfect stereochemical match suggests that this is a feature designed to optimize the enzyme's true physiological role, namely, to stabilize the transition state during hydrolysis of phospholipids condensed in micellar or lamellar aggregates. Indeed, the thermodynamic advantages afforded by the displacement of these water molecules (discussed above) would appear to require a constant stereochemistry at the catalytic surface rather than an allosteric change.

Of course, the interface could affect catalysis by altering the binding of substrate or cofactor. For example, it is possible that binding of the distal amino alcohol of the *sn-3* phosphate is influenced by the presence of nearby substrate molecules or that the interface mediates formation of enzyme oligomers. Several kinetic studies are compatible with models in which

PLA_2 forms dimers or higher order oligomers on the interface in order to exhibit full enzymatic activity (26). However, the role of enzyme aggregation is not obligatory since the same enzymes do not form oligomers on anionic vesicles during high levels of catalytic activity (27). In any case, there is nothing in our crystallographic work on the PLA_2-diC_8(2Ph)PE complexes to suggest how dimerization could enhance activity.

In the absence of allosteric modulation of the active site, how does interfacial binding "improve" the efficiency of PLA_2 catalysis? The crystal structures show that the catalytic event occurs on a rigid internal surface that is well shielded from bulk solvent. In our discussion of the hydrophobic channel and the interfacial recognition surface we suggest that the phospholipid molecule undergoing hydrolysis leaves the aggregate and reaches this catalytic surface by facilitated diffusion through a hydrophobic channel whose opening is in the interfacial binding surface (Fig. 6). Two factors facilitate this diffusion and optimize catalysis. First, the conformation of the substrate seen in the complexes is similar to that seen in crystalline aggregates (22) as well as that inferred by nuclear magnetic resonance experiments on phospholipids in micelles (28). This suggests that significant deformation is not required to achieve substrate transfer to the productive-mode binding site. In essence, the enzyme has evolved a mechanism for specificity that selects for the conformation imposed upon the phospholipid by the aggregate (7, 29, 30) and only substrates that can follow this access route are properly positioned for catalysis. This view is compatible with studies with covalently constrained substrates which indicate that substrate aggregation imposes on the phospholipid the conformation required for full susceptibility to PLA_2 action (7, 29). Thus it is the substrate's conformation that is influenced by phospholipid aggregation, rather than the enzyme's structure. Second, we visualize that because of the "seal" provided by interfacial binding, the transfer of substrate into the active site through the hydrophobic channel can occur without solvation of the hydrophobic alkyl substituents (Fig. 6). In addition to no torsional strains, there are also no solvation effects to raise the free energy during the transfer of the phospholipid from the aggregate to its binding site.

Thus the crystal structures suggest an isostructural, desolvated, and presumably isoenergetic transfer of phospholipid from the substrate aggregate to the catalytic surface through a hydrophobic channel whose opening is bound to the lipid-water interface. This access mode is required for optimal enzymatic action and can only occur at the interface. Soluble and dispersed phospholipids cannot exploit these features.

Acknowledgments

The research at Yale was supported by NIH grant no. GM22324 and by the Howard Hughes Medical Institute; the research at the University of Washington was supported by NIH grant no. HL36235. D.L.S. is a postgraduate fellow at Yale and a graduate student pro forma at the University of Chicago, and S.P.W. is a fellow of the Arthritis Foundation.

REFERENCES AND NOTES

1. Noel JP, Tsai MD. J Cell Biochem. 1989; 40:309. [PubMed: 2674160] de Geuss P, et al. Nucleic Acids Res. 1987; 15:3743. [PubMed: 3295782]
2. White SP, Scott DL, Otwinowski Z, Gelb MH, Sigler PB. Science. 1990; 250:1560. [PubMed: 2274787]
3. The subclasses refer to a large family of homologous sequences designated by Heinrikson et al. [Heinrikson RL, Krueger ET, Keim PS. J Biol Chem. 1977; 252:4313. [PubMed: 863929]] on the basis of small differences in disulfide distribution and certain sequence segments. Class I are from mammalian pancreas and elapid venom (such as *N. n atra*). Class II are from crotalid and viper venom. The family is referred to throughout this article as the Class I/II family.
4. Scott DL, Otwinowski Z, Gelb MH, Sigler PB. Science. 1990; 250:1563. [PubMed: 2274788]

5. When designating a functionally important residue the first number refers to the sequence position in the Class I/II family according to the common numbering system suggested by Renetseder et al. [Renetseder R, Brunie S, Dijkstra BW, Drenth J, Sigler PB. J Biol Chem. 1985; 260:11627. [PubMed: 4044572]] on the basis of structural similarity. The second entry is the corresponding sequence number in bee-venom PLA_2. The highly conserved His48 and Asp49 of active PLA_2 have been shown by chemical modification studies [His48—see (6); Asp49— Fleer EAM, Verheij HM, de Haas GH. Eur J Biochem. 1981; 113:283. [PubMed: 7202411]] and site-directed mutagenesis [Asp49—C. van den Bergh J, Slotboom AJ, Verheij HM, de Haas GH. J Cell Biochem. 1989; 39:379. [PubMed: 2722967]] to be critical to PLA_2 catalysis

6. Verheij HM, et al. Biochemistry. 1980; 19:743. [PubMed: 7356955]

7. Achari A, et al. Cold Spring Harbor Symp Quant Biol. 1987; 52:441. also unpublished data. [PubMed: 3454272]

8. Dijkstra BW, Drenth J, Kalk KH. Nature. 1981; 289:604. [PubMed: 7464926]

9. Since the structure of the uninhibited bee-venom PLA_2 is not known, the case for a similar catalytic mechanism is based on extrapolation of its nearly identical interaction with diC_8(2Ph)PE.

10. Dupureur CM, Deng T, Kwak JG, Noel JP, Tsai MD. J Am Chem Soc. 1990; 112:7074.

11. Blow D. Nature. 1990; 343:694. [PubMed: 2304545]

12. Wright CS, Alden RA, Kraut J. 1969; 221:235. ibid. Blow DM, Birkoft JJ, Hartley BS. :337. ibid.

13. Brady L, et al. 1990; 343:767. ibid. Winkler FK, D'arcy A, Hunziker W. :771. ibid.

14. Gandour R. Bioorg Chem. 1981; 10:169.

15. Strynadka NCJ, James MNG. Annu Rev Biochem. 1989; 58:951. [PubMed: 2673026]

16. Kuipers OP, Dijkman R, Pals CEGM, Verheij HM, de Haas GH. Protein Eng. 1989; 2:467. [PubMed: 2710783] Tsai PC, Hart J, Jaing RT, Bruzyk K, Tsai MD. Biochemistry. 1985; 24:3180. [PubMed: 3839681]

17. These water molecules have been observed in all high-resolution PLA_2 · calcium crystal structures.

18. Whereas the interaction of PLA_2 with *sn-2* amides and carbonyl esters can be observed directly, the binding mode of the true substrate can only be inferred from the structure of the bound transition-state analogue. Computational studies can be used to predict these binding modes and their stability.

19. Calcium ions are identified by the refinement assigning a compact density of 18 electrons to the site with a temperature factor consistent with the surrounding structure. Attempts to assign a water molecule to the same density cause the refinement to simulate a compact higher density by crystallographically assigning a physically unrealistic negative temperature factor. There is no way to confidently distinguish a calcium ion from the isoelectronic potassium ion; however, no potassium salts were used in the preparation or purification of the proteins, diC_8(2Ph)PE, or any of the crystal-stabilizing supernatant solutions.

20. A second calcium site has been noted in the porcine pancreatic enzyme. We do not know whether the displacement of calcium from the uninhibited form of the *N. n atra* enzyme on binding the transition-state analogue is physiologically relevant or an artifact caused by the high ammonium sulfate used to crystallize the inhibited form.

21. Dijkstra BW, Kalk KH, Hol WGJ, Drenth J. J Mol Biol. 1981; 147:97. [PubMed: 7265241] The crystal structure of bovine PLA_2 at 1.7 Å does not show a ligation cage for a secondary calcium. Lys122, which seemingly replaces the secondary calcium ion in the bovine enzyme, is conserved in all the mammalian pancreatic enzymes. The high-resolution structures of the Class II PLA_2 from the venom of *Crotalus atrox* and *Agkistridon piscivorus p. piscivorus* (A. Achari, D. L. Scott, S. Brunie, P. B. Sigler, unpublished observations) shows neither a supplemental calcium site nor an appropriately positioned basic side chain.

22. Elder M, Hitchcock P, Mason R, Shipley GG. Proc R Soc London Ser A. 1977; 354:157.Pearson RH, Pascher I. Nature. 1979; 281:499. [PubMed: 492310] Hauser H, Pascher I, Pearson RH, Sundell S. Biochem Biophys Acta. 1981; 650:21. [PubMed: 7020761]

23. Yoshida M, et al. J Biochem. 1988; 103:156. [PubMed: 3360757] Jain MK, Vaz WLC. Biochim Biophys Acta. 1987; 905:1. [PubMed: 3676302] Ludescher RD, et al. Biochemistry. 1988; 27:6618. [PubMed: 3219357]

24. Abita JP, Lazdunski M, Bonsen PPM, Pieterson WA, de Haas GH. Eur J Biochem. 1972; 30:37. [PubMed: 4673648] Pieterson MA, Volwerk JJ, de Haas GH. Biochemistry. 1974; 13:1455. [PubMed: 4819758]
25. The fourth conserved water in the Class I/II family ties the terminal amino group to the catalytic network by mediating hydrogen bonds between N1, O64, N52, and Oδ2 of Asp99. This water is not displaced from its position between Asp99 and the amino terminus.
26. Lombardo D, Dennis EA. J Biol Chem. 1985; 260:16114. [PubMed: 4066705] Romero G, Thompson K, Biltonen RL. 1987; 262:13476. ibid. Cho W, Tomasselli AG, Heinrikson RL, Kezdy FJ. 1988; 263:11237. ibid.
27. Jain MK, Berg O. Biochem Biophys Acta. 1989; 1002:127. [PubMed: 2649150]
28. Seelig JQ. Rev Biophys. 1977; 10:353.Hauser H, Phillips MC. Prog Surf Membr Chem. 1979; 13:297.
29. Barlow PN, Lister MD, Sigler PB, Dennis EA. J Biol Chem. 1988; 263:12954. [PubMed: 3417646]
30. Wells MA. Biochemistry. 1974; 13:2248. [PubMed: 4857565]
31. Yuan W, Gelb MH. J Am Chem Soc. 1988; 110:2665.
32. Yuan W, Quinn DM, Sigler PB, Gelb MH. Biochemistry. 1990; 29:6082. [PubMed: 2383571]
33. The coefficients of the Fourier sum are $(2F_o–F_c)\exp(i\,\varphi_c)$, where F_o is the observed amplitude and F_c and φ_c are the amplitude and phase, respectively, of the structure factors calculated from the refined model.
34. Fitzgerald PMD. J Applied Crystallogr. 1988; 21:273.
35. Otwinowski Z, et al. Nature. 1988; 335:321. [PubMed: 3419502]
36. Kossiakoff AA, Spencer SA. Biochemistry. 1981; 20:6462. [PubMed: 7030393]

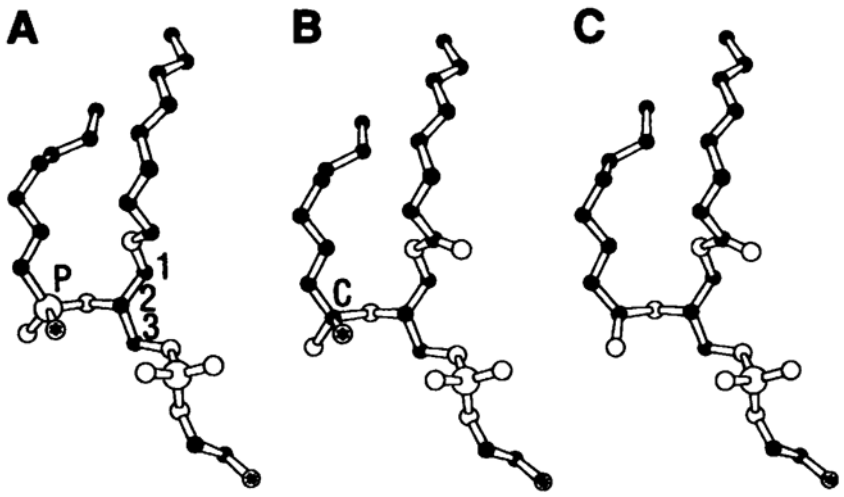

Fig. 1.

(**A**) The transition-state analogue, *L*- -l-*O*-octyl-*2*-heptyl-phosphonyl-*sn* -glycero-*3*-phosphoethanolamine, is a short-chain member of a class of strong PLA_2 inhibitors studied by Gelb and co-workers (31, 32) in which a phosphonate replaces the *sn-2* ester. This analogue was designed to emulate the transition state (**B**) formed in the hydrolysis of l,2-dioctanoyl-*sn-3*-phosphoethanolamine (**C**) and is therefore designated as $diC_8(2Ph)PE$. The conformation of $diC_8(2Ph)PE$ as seen in the complex with the PLA_2 from *N. n. atra* venom was used to model the structure of l,2-dioctanoyl-*sn*-3-phosphoethanolamine and its transition state; the ester carbonyls are shown with correct bond distances and interbond angles but their positions do not necessarily represent the minimum energy conformations. (C, P, O, and N atoms are represented by black spheres, large open spheres, small open spheres, and striped spheres, respectively; the spheres with asterisks denote the positions of the oxyanions.)

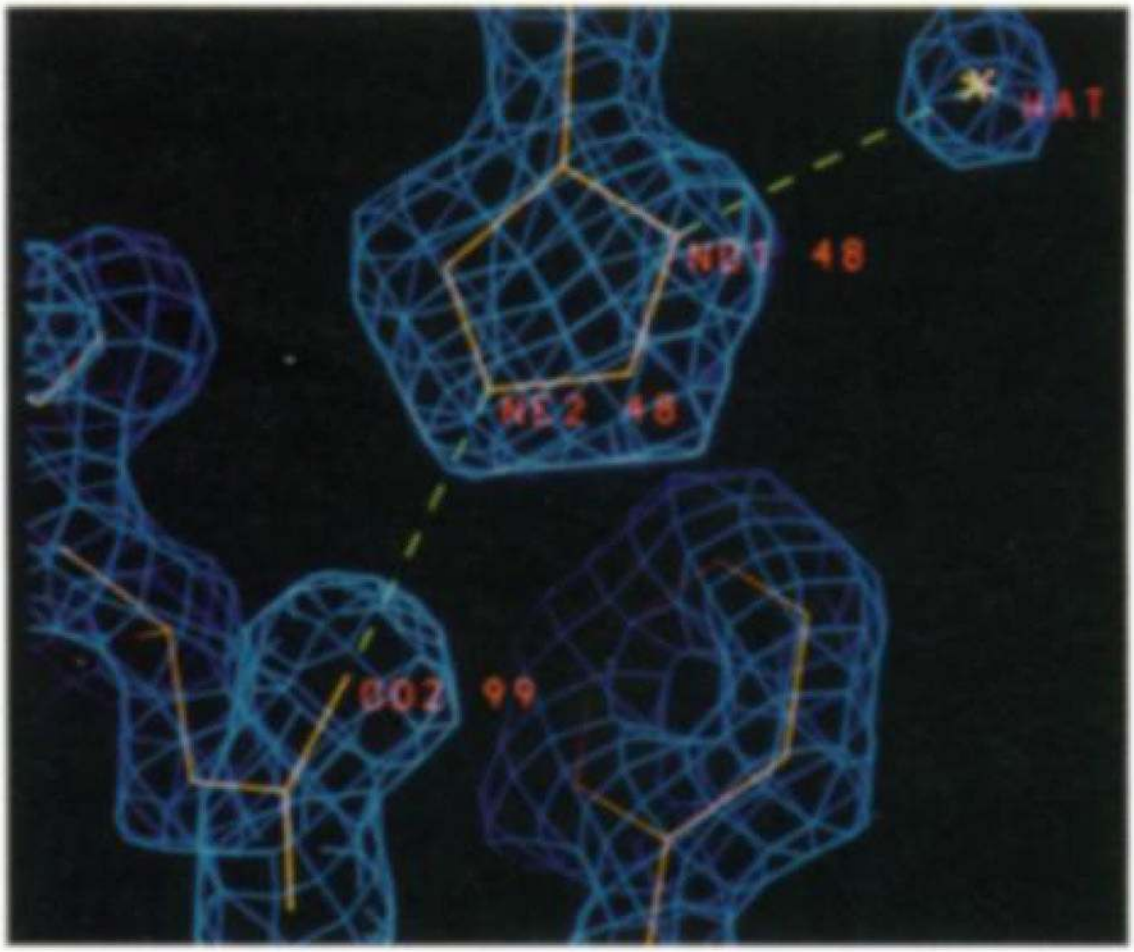

Fig. 2.

The structure of *N. n. atra* PLA_2; electron density map ($2F_o–F_c$) of the "attacking" water molecule from which His48 abstracts a proton (33). The enzyme was purified from crude venom (Miami Serpentarium) (32). Droplets (12 μl) containing 10 mg/ml protein, 10 mM $CaCl_2$, 0.1 M sodium cacodylate, 20 percent 1,4-butanediol, pH 6.8, were plated onto plastic cover slips and inverted over 1-ml reservoirs containing 0.1 M sodium cacodylate, 50 percent 1,4-butanediol, and 10 percent methyl alcohol. The crystals (0.4 mm by 0.2 mm by 0.2 mm) were of space group *I*4, $a = b = 93.0$ Å, and $c = 22.2$ Å, with one molecule in the asymmetric unit. Data to 1.5 Å resolution ($R_{sym} = 0.05$) were collected with two San Diego Multiwire System detectors; source radiation was graphite-monochromated CuK_α, emission from a Rigaku 300 x-ray generator. The structure was solved by molecular replacement with the program Merlot 1.5 (34) modified as described (35). The search molecule was the model of the same enzyme derived from the crystal structure of its complex with a phosphonate transition-state analogue (2). Refinement converged readily to an *R* factor of 0.143 for data in the resolution range 8.3 to 1.5 Å ($F > 1.5\ \sigma_F$). On average, bond lengths, bond angle distances, and planarity deviated from ideal values by less than 0.016, 0.031, and 0.021 Å, respectively.

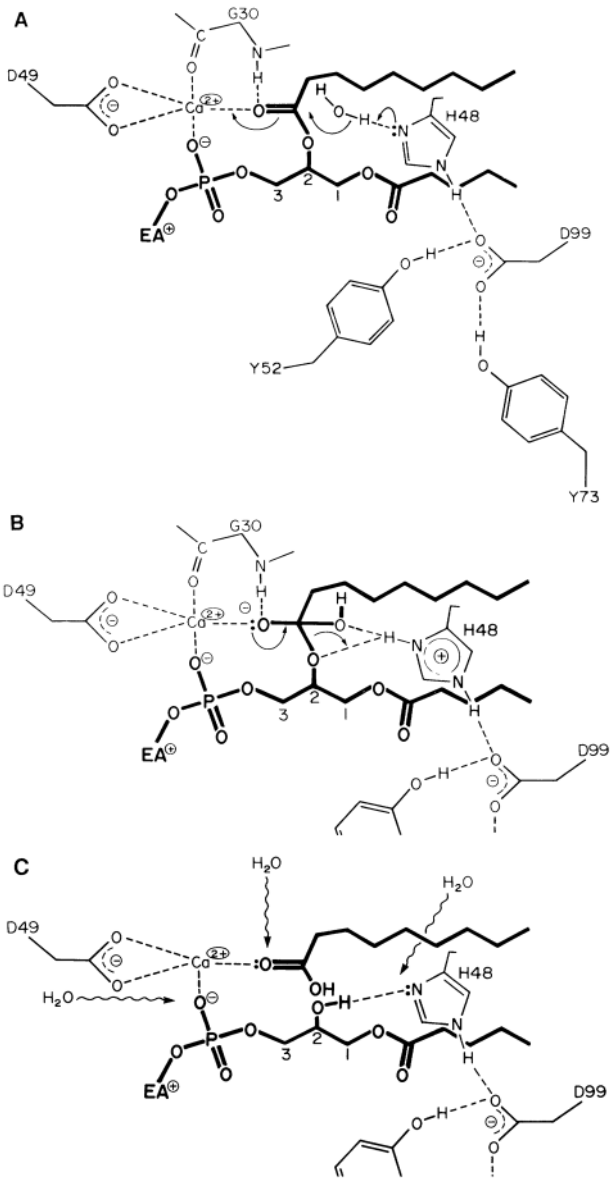

Fig. 3.

Catalytic mechanism. Residues of the Class I/II superfamily are used here for familiarity. They are replaced by Asp67, His34, and Tyr87 in the bee-venom enzyme. Although Tyr52 and Tyr72 are absolutely conserved in the Class I/II homologous superfamily they are not shown in (B) and (C). (**A**) Catalytic attack on substrate bound in a productive mode. The positions of the protons are not known but assumed from other catalytic systems (36). (**B**) The tetrahedral intermediate as it collapses into products. (**C**) The products formed by "productive collapse." Three water molecules move into the active site (as indicated by the arrows) to replace the products. One will engage the Nδ1 of His48, and the remaining two will coordinate the calcium ion (one equatorially and one axially).

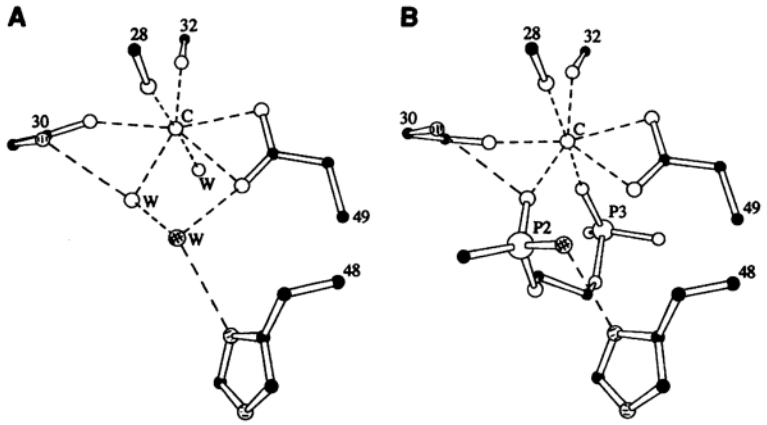

Fig. 4.

Interface between the transition-state analogue and the catalytic surface. (**A**) *Naja naja atra*–venom PLA_2; the catalytic surface in the absence of diC_8(2Ph)PE. Waters are labeled W, the primary calcium ion is labeled Ca, and the attacking nucleophile is cross-hatched. (**B**) *Naja naja atra*–venom PLA_2 (asymmetric unit "b"); P2 simulates the tetrahedral intermediate and P3 corresponds to the *sn-3* phosphate. The interaction in asymmetric unit "a" is identical, as is the bee-venom interface where Asp49(35) contributes the carboxylate; residues 28(8), 30(10), and 32(12) of the calcium-binding loop contribute backbone carbonyls to the calcium ligation cage. Atoms are identified as in (A).

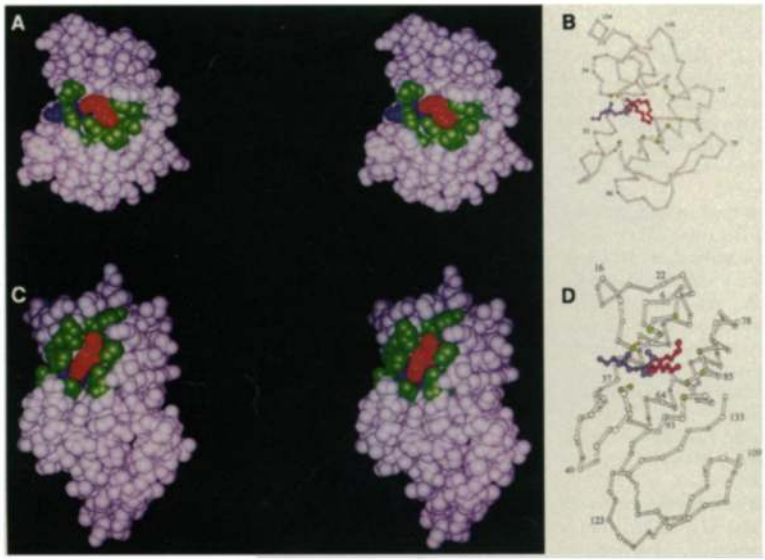

Fig. 5.

Complexes of diC_8(2PH)PE with PLA_2s. (**A** and **B**) *Naja naja atra*–venom PLA_2. (A) Van der Waal's surface showing the alkyl substituents of the phospholipid protruding from the surface (red) and surrounded in green by residues that form the "mouth" of the hydrophobic channel [Leu(Val)2, Phe5, Tyr6, Ile9, and Trp19] and by residues that have been shown to be [Tyr(Trp)3 and Trp19] or arc very likely to be [Lys6 and Arg31] part of the interfacial binding surface. The non-alkyl inhibitor elements are colored blue. (B) A skeletal representation of (A); the primary calcium ion is shown in yellow. (**C** and **D**) Bee-venom PLA_2. (C) Van der Waal's surface color-coded as above except that the residues of the mouth of the channel and the interfacial binding surface (green) are surmised from their proximity to the alkyl substituents or the enzyme surface or both [Ile1, Tyr3, Cys9, His11, Thr56, Arg57, Leu59, Val83, Met86, Tyr87, and Ile91]. (D) A skeletal representation of (C); the primary calcium ion is shown in yellow.

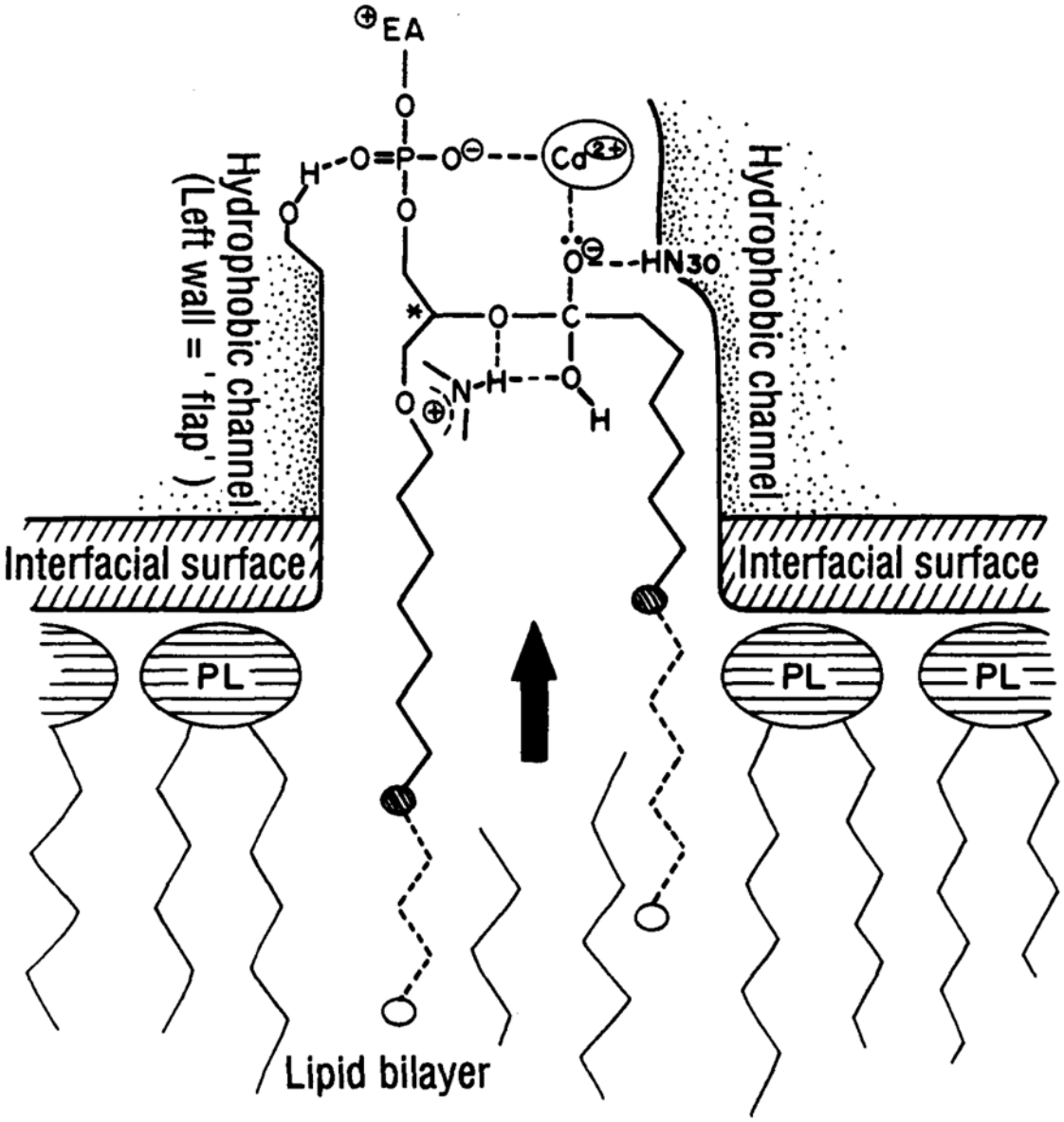

Fig. 6.
Schematic rendition of a productive interaction between a PLA_2 and aggregated substrate.